

LOCALIZATION OF METHANE SIGNALS IN GALE CRATER

M.A. Mischna, *Jet Propulsion Laboratory, California Institute of Technology, Pasadena, CA, USA* (michael.a.mischna@jpl.nasa.gov), **Y. Luo, J. Li, D. Adams, Y.L. Yung**, *Division of Geological and Planetary Sciences, California Institute of Technology, Pasadena, CA, USA*, **J. Lin, B. Fasoli**, *U. Utah, SLC, UT, USA*.

Introduction: The origin of methane in the Martian atmosphere has implications for geology, geochemistry, atmospheric chemistry and astrobiology. The Tunable Laser Spectrometer (TLS) onboard the Curiosity rover has detected several methane spikes during its multi-year operation in Gale crater on Mars. To better constrain the location of potential methane emission sites responsible for these signals, we have used several complementary numerical tools to identify approximate source locations given the timing and magnitude of the detected signals. Following from this work, we have since developed a multi-node detecting strategy that demonstrates what resources would be required to constrain the location of a source to within a region small enough for a present-day Mars rover to cover. Such an approach could be used to determine the highest priority future landing sites for studying the origin of Mars methane.

The work relies on the implementation of back-trajectory, Lagrangian numerical methods—an approach commonly used on Earth for tracking trace gas emissions. We use the Stochastic Time-Inverted Lagrangian Transport (STILT) model, in conjunction with the MarsWRF general circulation model (GCM) to trace viable upstream emission regions responsible for the detected signals.

Background: In the past two decades, multiple studies have sought to retrieve both the methane abundance in the martian atmosphere as well as its spatial distribution. Various techniques have reported quite variable abundances and distributions from orbital or remote observations [1-8]. The Tunable Laser Spectrometer (TLS) [9] on board the Curiosity rover was sent to Gale crater to make direct, in situ measurements at the martian surface. During 7.1 years of operation through January 2020, 36 distinct measurements have revealed a baseline level of ~ 0.41 parts-per-billion-by-volume (ppbv) [10], with episodic spikes up to ~ 21 ppbv [11] as summarized in Figure 1. These spikes have been interpreted as discrete, possibly proximate, methane emission events [10,12]. Concurrently, the ExoMars Trace Gas Orbiter (TGO) has been making solar occultation observations of methane concentration at mid- to high altitudes since 2018. However, it has reported a stringent upper limit of methane of only 0.02 ppbv [13-15], a result seemingly in conflict with the ground-based, TLS background observations of 0.41 ppbv.

Mechanisms have been proposed to reconcile this inconsistency. For example, TLS has performed all its measurements in the near-surface planetary boundary layer (PBL), and methane, if released from the surface, could accumulate in the shallow nighttime PBL [16,17]. Some speculative fast removal mechanisms

that can possibly cause temporal and spatial inhomogeneity of methane concentration have also been proposed [18-20]. In [21], the circumstances under which these discrepancies could be reconciled was studied, and the likelihood of these circumstances evaluated.

Inferring the location(s) of methane emission sites requires correct modeling of complex atmospheric transport processes. An early attempt to do so involved using a diffusion model to represent the spread of observed methane plumes [8], which was shown to be oversimplified when accounting for the importance of advection by bulk wind [22]. Separately, the Global Environmental Multiscale (GEM)-Mars GCM was used to simulate methane transport and then a statistical approach, based on the idea of simultaneous satisfaction of multiple observational constraints, was used for methane source localization [3]. Results suggested an emission region to the east of Gale crater for TLS's first methane spike (Spike 1 in Figure 1). Later, the Mars Regional Atmospheric Modeling System (MRAMS) mesoscale model was used to simulate the transport and dispersion of methane plumes emitted from 10 selected source regions around Gale crater [23]. Substantial dilution during tracer transport was observed, which demonstrated the importance of incorporating turbulent dispersion into tracer transport modeling. Among all the ten emission region candidates, the region to the northwest of the crater was favored, differing from the findings of [3].

In [21] the STILT model was used in conjunction with the MarsWRF GCM to identify upstream emission regions on the martian surface for seven observed methane spikes (through January 2020), finding that air from the northwestern crater floor had the strongest influence on the methane spike detections. Spikes 6 and 7 (Figure 1) were each observed in close temporal proximity to background measurements (labeled in Figure 1), providing additional information on source location, and suggesting an active emission site to the west or southwest of Curiosity on the northwest crater floor.

Approach and Results:

Localizing the Curiosity Signal: Using an inverse Lagrangian analysis for each of the seven detected plumes, [21] was able to establish a tie between the measured signal strength by Curiosity and upwind surface source locations—collectively known as the ‘footprint.’ In this approach, the STILT model transports an ensemble of 1000-10,000 air parcels backwards in time from the detector location, starting at the time of the atmospheric observation, following the winds generated by MarsWRF. The air parcels reveal the response of the measured trace gas concentration by TLS to all upwind surface source locations

(collectively, the “footprint”), in units of ppbv/($\mu\text{mol s}^{-1}$) [24]. The footprint captures the sensitivity of an atmospheric observation to surface fluxes upwind and is calculated by integrating and tallying air parcels over finite grid and time elements. Alone, the footprint tells of those upwind regions that will have, at a chosen prior time, the greatest influence on the instantaneous tracer concentration measured by the detector. When further multiplied by an a priori surface flux field (a constant regional emission over time, or an instantaneous point source being two example end-members) and integrated in space and time, the footprint will yield a mixing ratio at the detector site. By comparing the predicted and observed mixing ratios, we can accept or reject notional surface flux fields based upon the magnitude of their differences.

Figure 2 (left column) shows the time-integrated footprints of Spikes 1 and 2 from Figure 1. Spike 1 (top row), from an early-afternoon measurement, shows greater sensitivity to emission from sites to the north than from other directions, whereas Spike 2 (bottom row), from an overnight measurement, shows a broader footprint over the entire northwestern crater floor. This does not, however, instruct us on the amount of methane that was released at the source to produce a spike—that requires an assumption about the nature of the methane release. If one assumes an instantaneous methane emission at the exact prior time when each and every ‘pixel’ within the footprint had the strongest influence on the TLS methane measurement, that yields the *minimum* amount of methane that could be released from a source at that pixel and still produce an observed spike at Curiosity. This mass value is shown in the right column of Figure 2 and the left of the two color bars. Sources closer in proximity to Curiosity require a smaller total emission to generate the measured spike abundance.

From here, one may then convert this total emission into a comparable global mean signal (rightmost color bar), which helps constrain locations from which the source may arise. At some distance from Curiosity, the amount of emission required from a source would generate a global contribution that exceeds the rate of photochemical loss assuming a methane lifetime of ~ 300 years, and methane levels would increase (which is not observed). These more distant locations cannot be viable solutions for the source of the methane spikes.

A single sensor, like TLS, provides some insight into the source location, confirming it is local to Gale crater (as opposed to a source outside the crater), but only localizing it, typically, to a quadrant of the crater. Building on this approach, we have developed a strategy that uses multiple sensors to more tightly localize the signal source, while seeking to optimize the multi-sensor distribution so as to minimize cost, and maximize the likelihood of unambiguously isolating a methane source region such that it may be explored in situ.

A Multi-Detector Strategy: The right column of Figure 2 represents the mass of released methane that would be required for a single detector at the Curiosity location (red star) to be able to sense a methane ‘spike’ of some magnitude (we choose 5 ppbv—approximately the concentration of both Spikes 1 and 2), were that emission to originate from any location within the boundaries of the crater. The cooler colors close to the red star indicate that, from those locations, a smaller mass flux of methane ($\sim 10^0$ - 10^2 kg) would be required for the detector to sense ≥ 5 ppbv methane. Warmer colors, more distant from the detector, would require a mass flux many orders of magnitude greater in order to be sensed by the detector.

While Figure 2 shows a specific example for the Curiosity detector, we can easily generate similar mass footprint maps for a detector placed anywhere in Gale crater. The footprint pattern will be different for each case, but the approach is the same. Consider, now, 25 uniformly distributed, simultaneously operating detectors in Gale crater (black dots in Figure 3) all making coincident measurements (for example, at the time of one of the TLS spike measurements). If at least one detector out of these 25 detects a methane signal, then we can infer that there must have been an active methane source in or around Gale crater. We first examine one of the detectors that positively detected methane. Based on its mass footprint (e.g., Figure 2, right column) and the actual prescribed value of the methane spike (e.g., 5 ppbv), we can obtain the mass of released methane required to cause a spike at this detector, as a function of location throughout Gale crater. For each location (think ‘pixel’) within the crater, we compare this mass with the required mass of released methane for the other detectors that also sensed a methane spike and see if the difference is within a factor of 2. We may also compare this mass with the threshold mass of released methane for all detectors that did *not* detect a methane spike, and see if this mass is lower than the threshold mass. We select all the locations that satisfy the above criteria and remove locations with required mass larger than 10^6 kg, which is almost certainly too large to be a real methane source. The remaining locations are the possible sources of the methane signal.

Figure 3 shows an example of this localizing method. In this scenario, a detection is made in a northern winter afternoon. A mass of 5×10^4 kg methane is released over 10 days from the location shown by the blue diamond (and, of course, the detectors have no knowledge of the location of the source. Based on the prevailing circulation patterns, some of these sensors will detect a methane signal, and some will not). By applying our localization criteria for the 25 detectors (black dots), the possible locations of the methane source can be determined, and are marked as the small colored region in Figure 3. These are potential source locations consistent with the sense/no sense results of each of the 25 detectors. Essentially, if a source were located at the blue diamond, in this

season, and with the shown distribution of 25 sensors, the method would tell us fairly well (within ~ 10 km) the approximate location of the source and its magnitude (within $\sim 20\%$). Expanding this process by modeling release separately from every pixel in the domain, we can create a map showing where in the crater, and how well, source regions can be localized (Figure 4). Here, colors represent, for a methane source potentially located at each and every pixel in the image, how well the 25-sensor distribution could localize the source. For example, a source emitting from a location colored red could be localized only to within ~ 1000 km² (not very good), while a source in a blue location would be localized to within 1 km² or better. White regions are areas where none of the 25 sensors could detect an emission signal.

Separating the overall colored region into

categories according to how well the source location can be constrained (within an area of $\sim 1, 3, 10, 30$ km radius), we see in how much of Gale crater a source can be localized as a function of the number of sensors emplaced (Figure 5). A network of 25 sensors can localize a single 5 ppbv methane signal produced by a 10^5 kg emission to within ~ 10 km (orange curve) over $\sim 45\%$ of Gale crater, with diminishing returns for additional sensors. Two signals, in two different seasons with different circulation patterns, can increase this coverage to nearly 70% (Figure 6). An evenly distributed sensor array is chosen for simplicity of design; however, a priori knowledge of crater circulation could increase these probabilities by reorganizing the same number of sensors into locations where gaps (in white) are filled, or where the sensitivity is otherwise low (warmer colors).

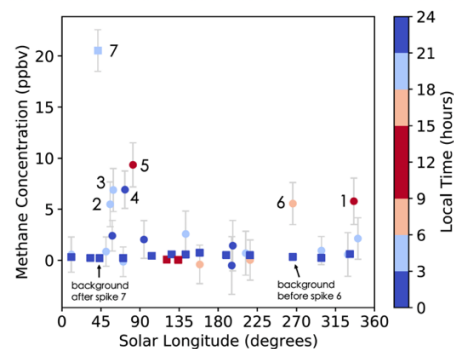


Figure 1: Tunable Laser Spectrometer methane signals versus Mars season and local time. The seven data points above 5 ppbv are regarded as “methane spikes” with their indices labeled. The 29 data points below 5 ppbv are regarded as the background abundance. Two background level measurements are also marked, one performed immediately before the detection of Spike 6 and the other after Spike 7. Direct-ingest measurements are shown in circles. Enrichment measurements are shown in squares. Colors show the local time of methane ingestions. Error bars show $\pm 1\sigma$ uncertainty. Adapted from [10,12].

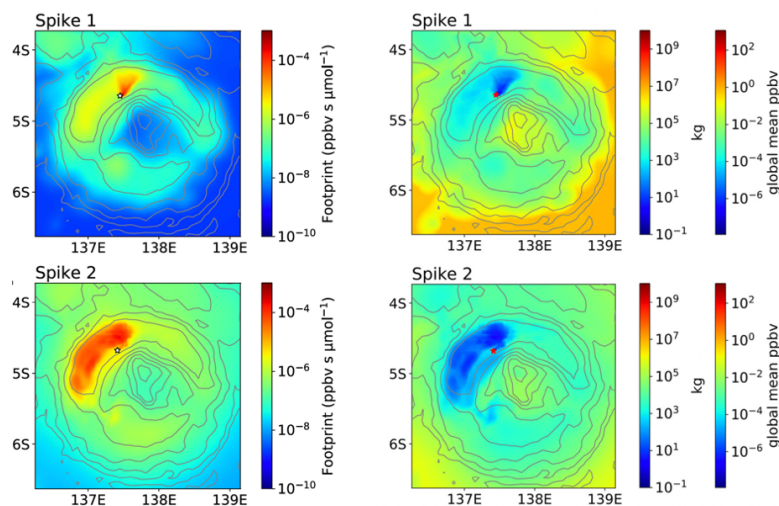


Figure 2 (left): Maps of time-integrated STILT footprint, showing the influence of any putative emission site on **(top)** Spike 1 and **(bottom)** Spike 2 at the Gale crater scale. High footprint values indicate strong upstream regions. **(right):** The minimum amount of methane emitted from every putative emission location (“pixel”) that can produce **(top)** Spike 1 and **(bottom)** Spike 2. For every pixel, an emission event is assumed to occur at the exact moment when that pixel has the strongest influence on a methane measurement by Curiosity. The left color bars show the minimum mass of emitted methane as required by the magnitude of the spikes. The right color bars show the increase in the globally averaged methane concentration after one of the aforementioned smallest emission event occurs. Contours show surface elevation. Stars mark the positions of Curiosity.

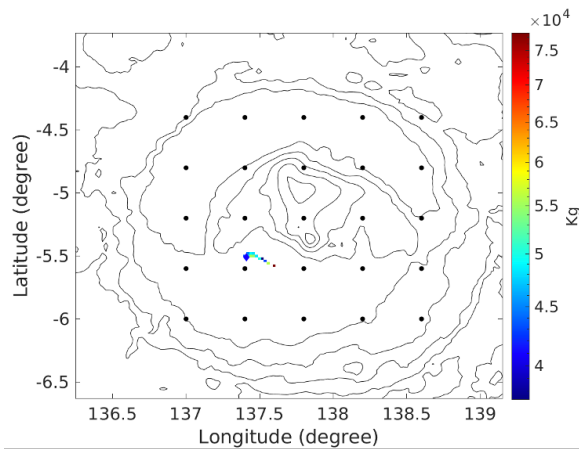


Figure 3: An example of the localizing method. Black dots indicate the position of the 25 sensors. The blue diamond represents the prescribed location of the methane source. The colored region shows the possible source locations, including the location of the blue diamond, derived from the localizing method.

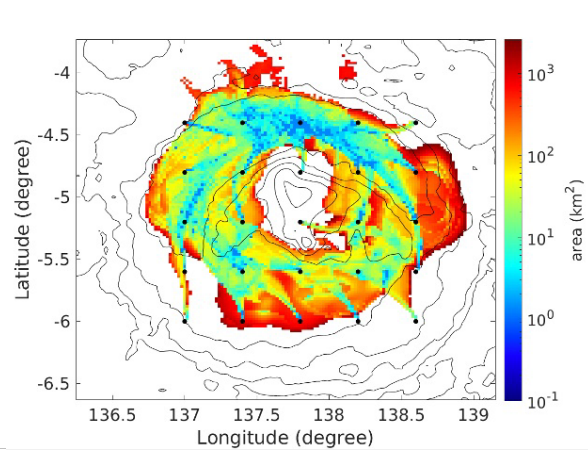


Figure 4: The area of possible locations derived by our method as a function of actual source location. The white region indicates areas where a methane source region could not be detected by any of the surface detectors. Pixels with cooler colors mean that a source location at that point would be well constrained, while pixels with warmer colors mean a source location at that point would be less-well constrained.

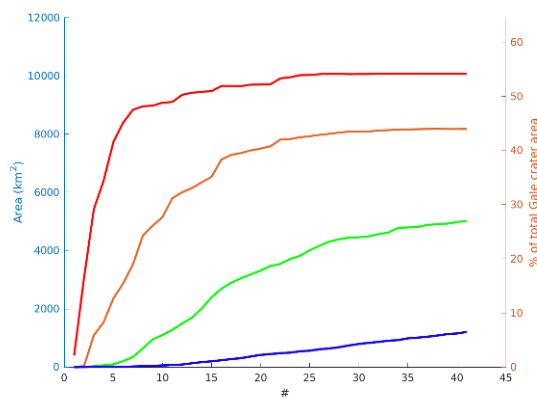


Figure 5: Sizes of four localization area categories (1, 3, 10, 30 km radius; blue, green, orange, red, respectively) as a function of the number of evenly distributed detectors, from 1 to 41, assuming a $\sim 10^5$ kg source emission. Up to 45% of Gale crater would have localization within 10 km.

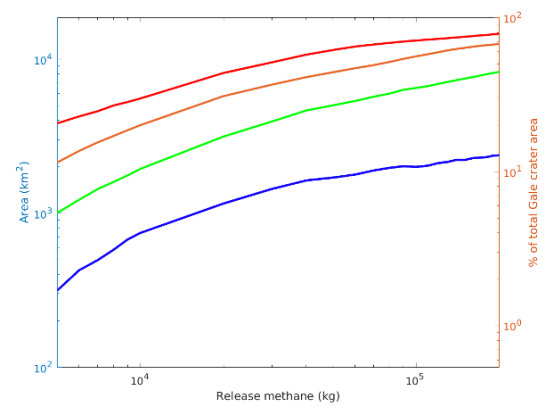


Figure 6: Area of possible source location covered by each of the four categories (as in Figure 5), but for two distinct detections at different seasons, with different atmospheric circulation patterns. For a 10^5 kg source emission, up to 70% of Gale crater would have localization within 10 km (orange curve).

References: [1] Aoki et al., 2018, doi:10.1051/0004-6361/201730903 [2] Geminale et al., 2008 doi:10.1016/j.pss.2008.03.004 [3] Giuranna et al., 2019 doi:10.1038/s41561-019-0331-9 [4] Fonti and Marzo, 2010 doi:10.1051/0004-6361/200913178 [5] Formisano et al., 2004 doi:10.1126/science.1101732 [6] Krasnopolsky 2012 https://doi.org/10.1016/j.icarus.2011.10.019 [7] Krasnopolsky et al., 2004 doi:10.1016/j.icarus.2011.10.019 [8] Mumma et al. 2009 doi:10.1126/science.1165243 [9] Mahaffy et al., 2012 doi:10.1007/s11214-012-9879-z [10] Webster et al., 2018 doi:10.1126/science.aaq0131 [11] Webster et al., 2021 doi:10.1051/0004-6361/202040030 [12] Webster et al., 2015 doi:10.1126/science.1261713 [13] Knutsen et al., 2021 doi:10.1016/j.icarus.2020.114266 [14] Korablev et al., 2019

doi:10.1038/s41586-019-1096-4 [15] Montmessin et al., 2021 doi:10.1051/0004-6361/202140389 [16] Moores et al., 2019 doi:10.1038/s41561-019-0313-y [17] Moores et al., 2019 doi:10.1029/2019GL083800 [18] Gough et al., 2010 doi:10.1016/j.icarus.2009.11.030 [19] Hu et al., 2016 doi:10.1089/ast.2015.1410 [20] Knak Jensen et al., 2014 doi:10.1016/j.icarus.2014.03.036 [21] Luo et al., 2021 doi:10.1029/2021EA001915 [22] Mischna et al., 2011 doi:10.1016/j.pss.2010.07.005 [23] Pla-García et al., 2019 doi:10.1029/2018JE005824 [24] Lin et al., 2003 doi:10.1029/2002JD003161